Threonyl-tRNA synthetase activates STAT3 by a nontranslational mechanism

Received for publication, July 19, 2025, and in revised form, November 13, 2025 Published, Papers in Press, December 9, 2025
https://doi.org/10.1016/j.jbc.2025.111032

Pallob Barai[1,‡], Reean Abdullah[1,‡], Shruti V. Bendre[2], Erin Weisser[2], Maxine J. van der Donk[3], Kent L. Wong[1], Adriana Reyes-Ordoñez[1], Erik R. Nelson[2,4,5,6,7], and Jie Chen[1,4,*]

From the [1]Department of Cell and Developmental Biology, and [2]Department of Molecular and Integrative Physiology, University of Illinois at Urbana-Champaign, Urbana, Illinois, USA; [3]Department of Chemistry, Northwestern University, Evanston, Illinois, USA; [4]Cancer Center at Illinois, [5]Beckman Institute for Advanced Science and Technology, [6]Carl R. Woese Institute for Genomic Biology- Anticancer Discovery from Pets to People, and [7]Division of Nutritional Sciences, University of Illinois at Urbana-Champaign, Urbana, Illinois, USA

Reviewed by members of the JBC Editorial Board. Edited by Karin Musier-Forsyth

Signal transducer and activator of transcription 3 (STAT3) is a major regulator of cell proliferation and survival, often found to be aberrantly activated in cancer. Here, we identify threonyl-tRNA synthetase 1 (TARS1) as an activator of STAT3. Elevated TARS1 expression in lung cancer correlates with poor patient survival. We find that overexpression of TARS1 supports non–small cell lung cancer cell proliferation *in vitro*, tumor formation of xenografts in mice, and hyperactivity of STAT3. Catalytically inactive TARS1 promotes STAT3 activation and cell proliferation, indicating that TARS1 functions in a nontranslational manner. Mechanistically, TARS1 physically associates with both STAT3 and Janus kinase (JAK), and TARS1 activation of STAT3 requires basal JAK activity. We propose a scaffold model in which TARS1 promotes proximity of STAT3 to JAK and subsequent phosphorylation of STAT3. This model is supported by the results of reconstitution experiments expressing recombinant TARS1, STAT3, and JAK1 in noncancer cells. Our study uncovers a novel mechanism of STAT3 dysregulation in cancer and provides a strong basis for therapeutic targeting of the noncanonical function of a housekeeping protein.

The signal transducer and activator of transcription (STAT) family of proteins are key transcription factors that regulate a wide array of cellular and developmental processes (1–4). Originally identified as the transcription factors responsible for interferon-responsive gene expression, STATs are phosphorylated and activated by Janus kinases (JAKs), a family composed of JAK1, JAK2, JAK3, and TYK2 (3, 5, 6). Upon cytokine binding to its cognate receptor, receptor-associated JAK becomes activated and phosphorylates receptor, which in turn recruits STAT to be phosphorylated by JAK. Phosphorylated STAT forms a dimer, translocates into the nucleus, and activates gene expression (1, 3, 6). STATs can also be activated directly by some receptor tyrosine kinases, such as epidermal growth factor receptor (EGFR) (7) as well as by the nonreceptor tyrosine kinase Src (8).

STAT3 plays multifaceted roles in biological processes ranging from embryogenesis to immunity and homeostasis of various tissues (9, 10). Y705 phosphorylation activates STAT3, and S727 phosphorylation modulates its activity (11). Notably, STAT3 is recognized as an oncogene because of its ability to drive oncogenic transformation both *in vitro* and *in vivo* when hyperactivated (12). Hyperactivation of STAT3 is found in many types of cancers, including breast, cervical, colon, pancreatic, ovarian, and lung cancers, as well as cancers of hematologic origin (13–15). Interleukin 6 (IL-6) is one of the most studied cytokines that activate STAT3 *via* JAK1, JAK2, or TYK2 (16), leading to the expression of genes that support cancer cell survival, proliferation, metastasis, and angiogenesis (16–18). More than 50% of non–small cell lung cancer (NSCLC) tumors and cell lines have elevated or constitutively active STAT3 (19). Potential upstream activators of STAT3 in lung cancer include IL-6, which has been reported to be constitutively produced in some lung cancer cell lines and lung cancer patients (20, 21), and EGFR, which is often overexpressed or mutated in the kinase domain in NSCLC cells (19). While the canonical mechanisms of STAT3 activation by receptors and JAKs are well characterized, there is potential for alternative modes of STAT3 activation or context-specific regulatory mechanisms given the ever-expanding complexity of the JAK–STAT signaling system (3).

Aminoacyl-tRNA synthetases (AARSs) are housekeeping enzymes that hydrolyze ATP and charge tRNAs with cognate amino acids, essential for protein synthesis (22). Numerous nontranslational functions of AARSs beyond the realm of protein synthesis have been identified, including regulation of gene expression, cytokine signaling, cell growth, angiogenesis, and inflammation (23–26). Threonyl tRNA synthetase 1 (TARS1), a class II cytoplasmic AARS, has been reported to have noncanonical functions (27). For instance, TARS1 can assemble a cap-dependent translation initiation complex (28). In an entirely different context, TARS1 negatively regulates skeletal muscle cell differentiation through inhibiting JNK

‡ These authors contributed equally to this work.
* For correspondence: Jie Chen, jiechen@illinois.edu.

signaling (29). In both cases, the N-terminal noncatalytic UNE-T domain is critical for the functions of TARS1 (28, 29). In addition, TARS1 is found to be secreted by human vascular endothelial cells upon vascular endothelial growth factor stimulation, and exogenous TARS1 can stimulate endothelial cell migration and angiogenesis, although a molecular mechanism is not known (30). Our current study uncovers a novel mechanism of STAT3 activation by TARS1, which may operate in cancer as well as noncancer cells.

Results

TARS1 promotes cell proliferation and tumor formation in a nontranslational mechanism

In perusing the Human Protein Atlas (https://www.proteinatlas.org/) (31), we noticed that TARS1 mRNA expression is elevated in several NSCLC cell lines. We also found that TARS1 overexpression inversely correlated with lung cancer patient overall survival (Kaplan–Meier plot: https://kmplot.com/analysis/) (32). Notably, although seven other AARSs displayed a similar correlation, the others did not (Fig. S1). This observation implies that the canonical protein synthesis role of AARS may not underlie the correlation between AARS overexpression and lung cancer patient outcome.

To probe a potential function of overexpressed TARS1, we chose several NSCLC cell lines with diverse levels of TARS1 mRNA expression based on information in the Human Protein Atlas and examined TARS1 protein expression by Western blotting. As shown in Figure 1*A*, TARS1 protein levels were found to be elevated in A549, H2170, H1703, and H520 cells compared with human embryonic kidney 293 (HEK293) cells and significantly lower in H226 cells. To examine a correlation between TARS1 expression and cell proliferation, we knocked down TARS1 using a previously published lentivirus-delivered shRNA (29). A significant reduction in cell number was found upon TARS1 knockdown in H1703 and H520 cells (Fig. 1*B*). TARS1 protein levels were reduced to ∼10% to 40% by the shRNA, and it is important to note that the degree of TARS1 knockdown was not higher in H1703 and H520 than in the other cell lines (Fig. S2*A*). To assess whether the reduction in cell number was due to inhibited cell proliferation or increased cell death, we performed 5-ethynyl-2′-deoxyuridine (EdU) labeling assay and TUNEL assay in H1703 cells 24 and 48 h after TARS1 was sufficiently knocked down (3 days of puromycin selection following lentivirus transduction; Fig. S2*B*). The numbers of proliferating and apoptotic cells were significantly reduced (Fig. 1*C*) and increased (Fig. 1*D*), respectively. Since shTARS1 reduced proliferating cells from ∼40% to ∼20% and increased apoptotic cells only by 1% to 2%, the effect of TARS1 knockdown on overall cell numbers was primarily because of a reduction in cell proliferation.

The cell phenotype of TARS1 knockdown could have resulted from compromised global protein synthesis. To

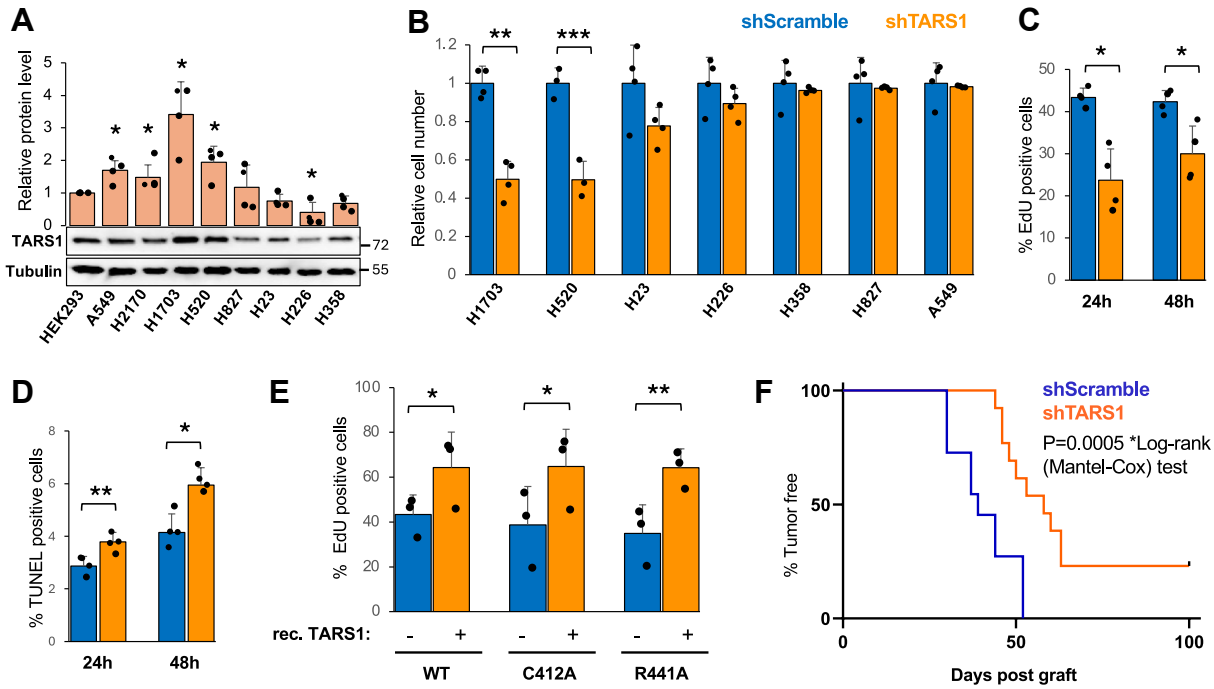

Figure 1. TARS1 knockdown inhibits cell proliferation in a nontranslational manner. *A,* TARS1 protein levels were analyzed by Western blotting and quantified. Data were normalized against HEK293 (N = 4). *B,* cells were transduced with lentiviruses and selected in puromycin for 4 days. Cell viability data were normalized to control for each line (N = 4). *C* and *D,* H1703 cells were transduced with lentiviruses and selected in puromycin for 3 days, followed by EdU assay (*C*) or TUNEL assay (*D*) after 24 and 48 h (N = 4). *E,* H1703 cells transduced with shTARS1 lentivirus and selected in puromycin for 2 days were transfected with WT or mutant TARS1 for 3 days, followed by EdU assay (N = 4). *F,* H1703 cells transduced with lentiviruses and selected in puromycin for 4 days were grafted into mice. Tumor formation was monitored over time (N = 12 for each condition), with data presented in the Kaplan–Meier survival curve. Statistical analyses: one-sample *t* test for *A* and *B*; paired *t* test for C–E. *$p < 0.05$, **$p < 0.01$. EdU, 5-ethynyl-2′-deoxyuridine; HEK293, human embryonic kidney 293 cell line; TARS1, threonyl-tRNA synthetase 1.

investigate that possibility, we made use of two mutants of TARS1 (C412A and R441A) that were expected to be catalytically inactive (29, 33). Aminoacylation assays with immunoprecipitated recombinant proteins confirmed that the R441A mutant had drastically reduced activity, whereas the C412A mutant activity was variable and not significantly different from the WT (Fig. S3). In TARS1 knockdown H1703 cells, expression of WT recombinant TARS1 (mouse complementary DNA, resistant to the shRNA) promoted proliferation as revealed by EdU assays, and each of the TARS1 mutants also promoted cell proliferation to the same extent as WT (Fig. 1*E*). At least, the result of R441A suggests that TARS1 has a role in promoting cancer cell proliferation through a nontranslational mechanism.

To probe the role of TARS1 in promoting cancer cell growth *in vivo*, we performed mouse xenograft experiments by grafting nude mice with H1703 cells treated with shTARS1 or shScramble lentivirus. We found that mice that were injected with TARS1 knockdown cells took longer to form palpable tumors than mice injected with control cells (Fig. 1*F*). Furthermore, while all the mice injected with control H1703 cells developed tumors, 23% of the mice injected with TARS1 knockdown cells did not form any tumor within 100 days of grafting (Fig. 1*F*). We observed no difference in histological features of the shScramble and shTARS1 tumors (Fig. S4). These observations indicate that tumor formation from the NSCLC cell line H1703 is dependent on elevated levels of TARS1.

TARS1 promotes STAT3 activation

To decipher the molecular mechanism by which TARS1 regulates cell proliferation nontranslationally, we set out to study the effect of TARS1 knockdown on signaling pathways commonly known to control cell proliferation. We performed experiments in the two NSCLC cell lines in which TARS1 knockdown inhibited cell growth—H1703 and H520 (Fig. 1*B*). A549 cells, which were not affected by the knockdown, were also included for comparison. The activity levels of the following signaling proteins were examined by Western blotting for their phosphorylation: ERK, p38, AKT, mTORC1 (S6K1), and STAT3. Previously, we had reported TARS1 regulation of JNK signaling in myoblasts (29), but phospho-JNK was not detected reliably in these NSCLC cells. The only consistent change observed in both H1703 and H520 (but not A549) cells was with STAT3; Y705 phosphorylation, which is critical for STAT3 dimerization and activation, was significantly diminished by TARS1 knockdown (Figs. 2*A* and S5). S727 phosphorylation of STAT3 was not affected.

As expected, expression of recombinant WT-TARS1 restored the level of pY705-STAT3 in H1703 cells with endogenous TARS1 knocked down (Fig. 2*B*). Importantly, the catalytically inactive mutants of TARS1, C412A, and R441A

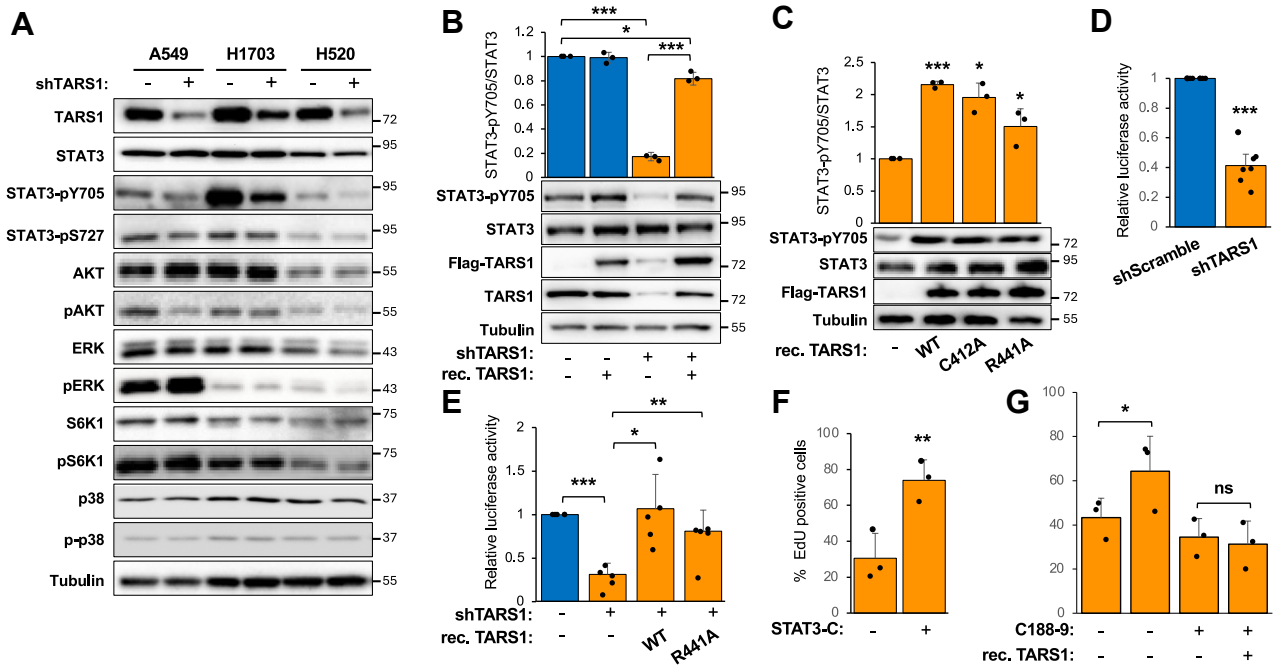

Figure 2. TARS1 knockdown inhibits STAT3 activity. *A,* cells were transduced with shScramble (–) or shTARS1 (+) lentivirus and selected in puromycin for 4 days, followed by Western blot analysis. N = 3. Quantification is shown in Figure S5. *B,* H1703 cells were transduced with lentiviruses as in *A* and selected in puromycin for 2 days, followed by transfection of TARS1 for 3 days and Western blot analysis. Data were normalized to control (N = 3). *C,* H1703 cells transduced with shTARS1 lentivirus were treated as in *B*, followed by Western blot analysis. Data were normalized to control (N = 3). *D,* H1703 cells were transduced with lentiviruses, selected in puromycin for 2 days, and transfected with a STAT3 reporter for 2 days, followed by luciferase assays (N = 7). *E,* H1703 cells were treated as in *D*, but the STAT3 reporter was cotransfected with TARS1. Luciferase assay was performed (N = 5). *F,* H1703 cells were treated as in *C* and transfected with STAT3-C for 3 days, followed by EdU assay (N = 4). *G,* H1703 cells were treated as in *B*, with 2.5 μM C188-9 for the last 24 h, followed by EdU assay (N = 3). Data without inhibitor were the same as in Figure 1*E*. Statistical analyses: two-way ANOVA followed by Tukey's post hoc test for *B* and *E*; one-sample *t* test for *C* and *D*; paired *t* test for *F* and *G*. *$p < 0.05$, **$p < 0.01$, and ***$p < 0.001$. EdU, 5-ethynyl-2′-deoxyuridine; STAT3, signal transducer and activator of transcription 3; TARS1, threonyl-tRNA synthetase 1.

also activated pY705-STAT3 (Fig. 2*C*), consistent with the notion that the effect of TARS1 on STAT3 is through a nontranslational mechanism. Next, we measured transcriptional activity of STAT3 using a luciferase reporter (34). Our results showed that TARS1 knockdown drastically reduced STAT3 reporter activity in H1703 cells (Fig. 2*D*) and that expression of WT-TARS1 or catalytically inactive mutant TARS1 (R441A) rescued the activity (Fig. 2*E*). Finally, to ascertain the role of STAT3 in mediating TARS1 regulation of cell proliferation, we expressed the constitutively active STAT3-C (12) in TARS1 knockdown H1703 cells. Indeed, we observed that STAT3-C enhanced proliferation of TARS1-knockdown cells (Fig. 2*F*). On the other hand, in the presence of the STAT3 inhibitor C188-9, TARS1 overexpression no longer promoted proliferation (Fig. 2*G*). Taken together, our observations strongly suggest that TARS1 activates STAT3 in a nontranslational manner to promote cell proliferation.

TARS1 interacts with STAT3

To elucidate the mechanism by which TARS1 regulates STAT3, we tested the possibility of physical interaction between the two proteins. We found that endogenous TARS1 and STAT3 interacted in coimmunoprecipitation (co-IP) experiments performed with H1703 cell lysates (Fig. 3*A*). This interaction was further confirmed by co-IP of recombinant proteins expressed in HEK293 cells: IP of FLAG-TARS1 brought down GFP-STAT3 (Fig. 3*B*) and IP of FLAG-STAT3 brought down GFP-TARS1 (Fig. 3*C*). We went on to map the domain of TARS1 responsible for the interaction by testing several truncation constructs (Fig. 3*D*). As shown in Figure 3*E*, deletion of the TGS (ThrRS, GTPase, and SpoT) domain, editing domain (ED), or anticodon-binding domain (ABD) did not affect TARS1 interaction with STAT3. On the other hand, a C-terminal truncation, which removed the aminoacylation domain (AAD) and ABD, abolished interaction with STAT3, suggesting that AAD is necessary for TARS1 interaction with STAT3. We were not able to test whether AAD is sufficient for interaction with STAT3 because AAD alone did not express well in cells.

Given our observation that the interaction with STAT3 involved TARS1's catalytic core domain, which is conserved among class II AARSs, we asked whether other AARSs may also interact with STAT3. To that end, we tested recombinant aspartyl-tRNA synthetase 1 (class II), lysyl-tRNA synthetase 1 (class II), leucyl-tRNA synthetase 1 (class I), and glutamyl-prolyl-tRNA synthetase 1 (dual enzyme) in co-IP experiments with recombinant STAT3. As shown in Figure 3*F*, none of those AARSs was pulled down by FLAG-STAT3. Therefore, interaction with STAT3 appears to be a feature unique to TARS1 among the AARSs.

TARS1 acts as a scaffold to activate STAT3 through JAKs

Next, we asked which kinase might be responsible for STAT3 phosphorylation promoted by TARS1 in NSCLC cells. JAK1 and JAK2 have been reported to be upstream of STAT3 in various NSCLC cells (35–37). Indeed, the pan-JAK inhibitor momelotinib (38) inhibited pY705 of STAT3 in H1703 cells in a dose-dependent manner (Fig. 4*A*). However, TARS1 knockdown did not affect the activity of JAK2 in H1703 or H520 cells (Fig. 4*B*). We were not able to detect JAK1 activity, which could be due to a low level of pJAK1 in these cells and/or low avidity of the antibody used. IL-6 is known to activate STAT3 in many NSCLC cells, but IL-6 treatment did not markedly increase the level of pY705-STAT3 in H1703 cells (Fig. S6*A*), most likely because STAT3 was already hyperactivated in these cells. This observation is consistent with the reported IL-6 independence of H1703 cells (35). Interestingly, IL-6 fully protected pSTAT3 from TARS1 knockdown (Fig. S6*A*), suggesting that IL-6 is capable of activating STAT3 in H1703 and that this activation is independent of TARS1. Furthermore, we found that serum

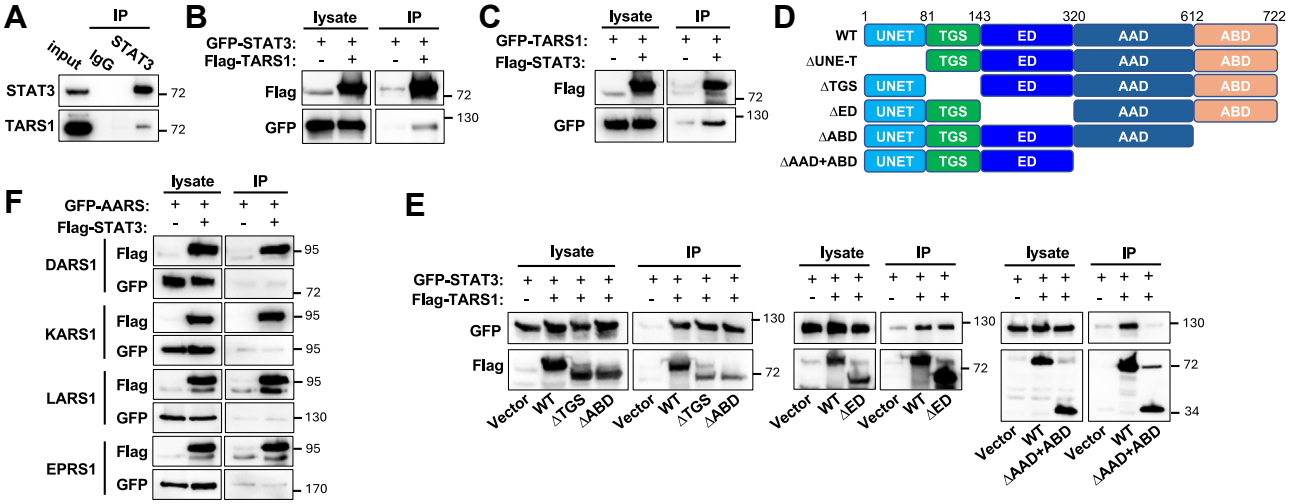

Figure 3. TARS1 physically interacts with STAT3. *A*, H1703 cells were subjected to immunoprecipitation (IP) with anti-STAT3 followed by Western blotting. N = 2. *B*, *C*, *E*, *F*, HEK293 cells were transfected for 2 days with various constructs as indicated, followed by anti-FLAG IP and Western blotting. N = 3. *D*, TARS1 domains and the truncation constructs used in this study. DARS1, aspartyl-tRNA synthetase 1; EPRS1, glutamyl-prolyl-tRNA synthetase 1; HEK293, human embryonic kidney 293 cell line; KARS1, lysyl-tRNA synthetase 1; LARS1, leucyl-tRNA synthetase 1; STAT3, signal transducer and activator of transcription 3; TARS1, threonyl-tRNA synthetase 1.

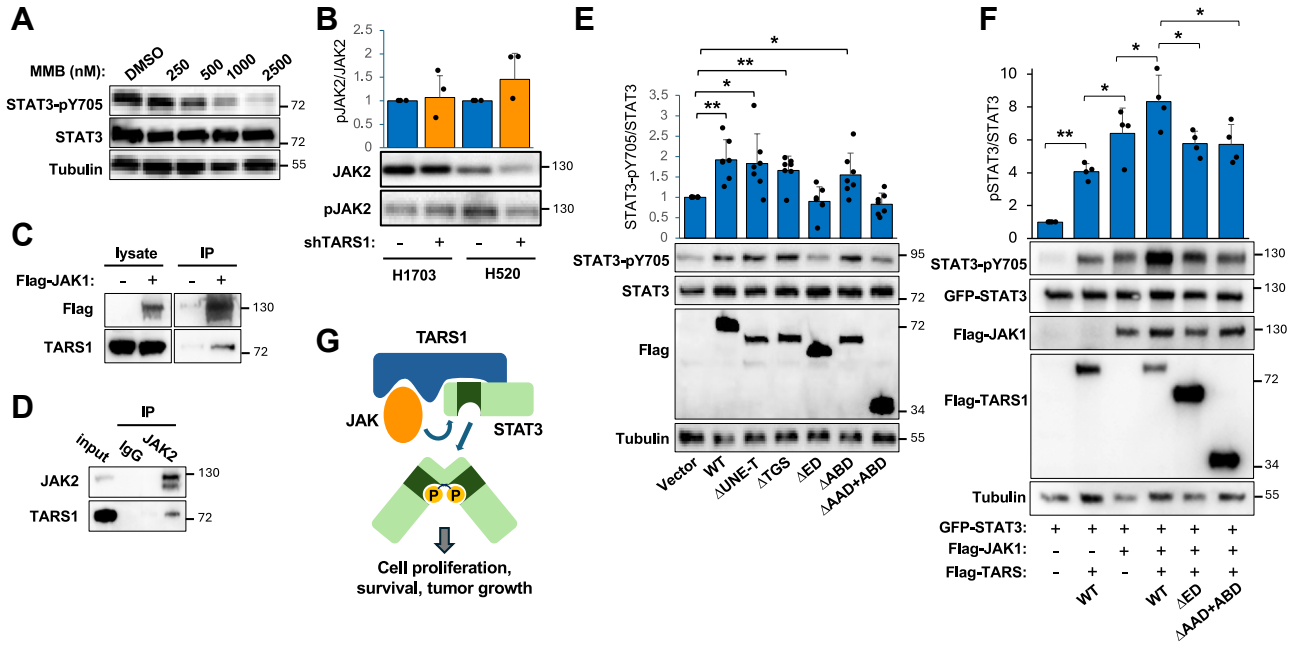

Figure 4. TARS1 act as a scaffold to activate STAT3 by JAKs. *A,* H1703 cells were treated with momelotinib (MMB) at concentrations indicated or dimethyl sulfoxide (DMSO) for 30 min, followed by Western blotting. N = 3. *B,* H1703 and H520 cells were transduced with shScramble (–) or shTARS1 (+) lentivirus and selected in puromycin for 4 days, followed by Western blotting and quantification (N = 3). *C,* HEK293 cells were transfected with FLAG-JAK1 (or empty vector) for 2 days, followed by anti-FLAG immunoprecipitation (IP). Endogenous TARS1 was detected by Western blotting. N = 3. *D,* H1703 cells were subjected to IP with anti-JAK2 followed by Western blotting. N = 2. *E,* H1703 cells were transduced with shTARS1 lentivirus and selected in puromycin for 2 days, followed by transfection with various TARS1 constructs for 3 days. Western blots were quantified, and the data were normalized against vector control (N = 7). *F,* HEK293 cells were cotransfected with various combinations of GFP-STAT3, FLAG-JAK1, and FLAG-TARS1 (WT or mutants) for 2 days, followed by Western blotting. Quantification data were normalized against GFP-STAT3 transfection alone (N = 4). *G,* a proposed model of TARS1 serving as a scaffold to activate STAT3. Statistical analyses: one-sample *t* test for *B* and *E*; paired *t* test for *F*. $*p < 0.05$, $**p < 0.01$. HEK293, human embryonic kidney 293 cell line; JAK, Janus kinase; STAT3, signal transducer and activator of transcription 3; TARS1, threonyl-tRNA synthetase 1.

starvation did not affect pSTAT3 status in H1703 cells (Fig. S6*B*), ruling out any stimulatory factor in the serum to be responsible for the hyperactivity of STAT3. Taken together, our observations suggest that TARS1 activation of STAT3 is most likely dependent on the constitutive activity of JAK and independent of cytokine receptor signaling.

A simple model that could explain all our observations thus far would be that, when overexpressed such as in certain NSCLC cells, TARS1 serves as a scaffold to bring JAK and STAT3 into proximity, thus promoting STAT3 phosphorylation and activation by JAK. Consistent with this model, a recombinant JAK1 pulled down endogenous TARS1 in a co-IP assay (Fig. 4*C*). Importantly, IP of endogenous TARS1 also brought down endogenous JAK2 from H1703 cells (Fig. 4*D*). To test the scaffold model functionally, we examined the capacity of various TARS1 truncations to activate STAT3 by expressing the recombinant proteins in TARS1-knockdown H1703 cells, similar to the experiments described earlier (Fig. 2, *B* and *C*). As shown in Figure 4*E*, the UNE-T, TGS, and ABD domains were dispensable for TARS1's effect on STAT3, whereas constructs lacking either ED or AAD no longer activated STAT3. Since AAD but not ED was involved in interacting with STAT3 (Fig. 3*E*), the requirement of ED for STAT3 activation suggests that ED may interact with JAK.

To further test our proposed model, we carried out a reconstitution experiment in HEK293 cells by expressing GFP-STAT3, FLAG-TARS1, and FLAG-JAK1. Expression of recombinant TARS1 enhanced phosphorylation of GFP-STAT3 (Figs. 4*F* and S7). Importantly, the JAK inhibitor (momelotinib) abolished TARS1-induced elevation of pSTAT3 (Fig. S7), suggesting that TARS1 activation of STAT3 is dependent on JAK. Overexpression of TARS1 also boosted recombinant JAK1 activation of pSTAT3, but the TARS1 mutants missing ED or AAD + ABD domains did not have any effect (Fig. 4*F*). Taken together, these observations are in full agreement with the scaffold model by which TARS1 promotes JAK activation of STAT3 (Fig. 4*G*).

Discussion

Our study unveils a novel mechanism of STAT3 activation by TARS1. In some NSCLC cells where TARS1 expression is elevated, cell proliferation is dependent on the overexpressed TARS1. TARS1 knockdown in H1703 cells drastically reduces tumor formation and growth in a xenograft mouse model, consistent with poor patient survival in lung cancer with high TARS1 expression. Our biochemical analyses have led us to propose that the activation of STAT3 by TARS1 is dependent on basal activity of JAK, and that TARS1, acting in a non-translational manner, serves as a molecular scaffold to enhance JAK phosphorylation of STAT3. Constitutively active or hyperactive STAT3 is found in many lung cancers. An important question is why not all the TARS1-overexpressing NSCLC cell lines we studied are dependent on TARS1 for

STAT3 activity and cell proliferation. Both H1703 and H520 are derived from squamous cell carcinoma, which is a less common type of NSCLC than adenocarcinoma. Common drivers in lung adenocarcinoma (but not lung squamous cell carcinoma) include EGFR and K-Ras mutations, which can serve as the activating signal upstream of STAT3. The H1703 and H520 cells, in which TARS1 is found responsible for STAT3 constitutive activity, do not harbor either EGFR or K-Ras mutation (DepMap (39)), and they do not express notable levels of IL-6 (The Human Protein Atlas (31)) for autocrine signaling. Hence, it is tempting to speculate that overexpressed TARS1 may provide the alternative means to activate STAT3 in NSCLC cells without EGFR and K-Ras mutations. Future investigation taking advantage of resources such as the Cancer Dependency Map (39) and a recently developed deep learning model (40) can lead to a broader understanding of TARS1's role in cancer.

Nontranslational functions of AARSs are often facilitated by appended domains outside the catalytic core of these enzymes (24, 41). Previously, we reported that TARS1 regulates JNK signaling through its appended domains (UNE-T and TGS) (29). However, in the current study, we find that those domains of TARS1 are dispensable for the activation of STAT3. Instead, the catalytic ED and AAD of TARS1 are necessary to exert the scaffolding function. The AAD (but not ED) is structurally conserved among class II AARSs (42), but we did not find STAT3 to interact with other AARSs tested (Fig. 3*F*). Therefore, it is conceivable that activation of STAT3 *via* a scaffolding mechanism is a unique function of TARS1, not shared by other AARSs. Several other AARSs also exhibit a strong correlation between their expression levels and lung cancer mortality (Fig. S1), and the underlying mechanisms will warrant future investigation. Targeting nontranslational functions of these house-keeping enzymes could offer novel anticancer strategies.

Data from our reconstitution experiments expressing recombinant TARS1, STAT3, and JAK in HEK293 cells also suggest that the scaffolding mechanism does not require a cancer-specific cellular context. It is likely that activation of STAT3 can occur under physiological conditions where the optimal concentrations of TARS1–STAT3–JAK are present to favor the scaffolding complex assembly. Identification of the types of cells, tissues, and physiological contexts in which TARS1 activates STAT3 can potentially lead to new biological insights. Although our current model does not involve receptor signaling, it is noted that JAK is often constitutively associated with cytokine receptors, raising intriguing questions that can guide future mechanistic dissections. For instance, what is the subcellular location where TARS1 functions as a scaffold? Are cytokine receptors involved in a ligand-independent manner?

Experimental procedures

Antibodies and plasmids

All antibodies used in this study were obtained from commercial sources (see supporting information for details). The sources or creation of plasmids are detailed in supporting information.

Cell culture

Cells were maintained in Ham's F-12K medium (for A549), RPMI1640 medium (for all other NSCLC cell lines), or Dulbecco's modified Eagle's medium (for HEK293), containing 4.5 g/l glucose, 10% fetal bovine serum, and 1% penicillin–streptomycin. All cells were cultured at 37 °C with 5% CO_2. Transfection of H1703 and HEK293 cells was performed using Lipofectamine 3000 and polyethylenimine, respectively. See supporting information for details.

Lentivirus-delivered RNA interference

shRNAs in the pLKO.1-puro vector were purchased from Sigma–Aldrich (MISSION The RNAi Consortium). shRNA details, lentiviral packaging, and viral transduction are described in supporting information.

Cell viability assay, cell proliferation assay, TUNEL assay, luciferase assay, and immunofluorescence staining

See supporting information for details.

Mouse xenograft

All protocols involving animals were approved by the Institutional Animal Care and Use Committee at the University of Illinois at Urbana-Champaign. See supporting information for details of the procedure performed.

Cell lysis, IP, and Western blotting

See supporting information for details.

Statistical analysis

All quantitative data were presented as mean ± SD. Statistical significance of the data comparison was analyzed by performing two-tailed paired, unpaired, or one-sample *t* test, or two-way ANOVA followed by Tukey's post hoc test for multiple comparisons. Differences between groups were considered significant when $p < 0.05$. The analyses were performed using Excel (Microsoft) and GraphPad Prism 8.0 (GraphPad Software, Inc).

Data availability

All supporting information are included in the main article and its supporting information.

Supporting information—This article contains supporting information (12, 29, 43–50).

Acknowledgments—We thank Mr Chong Dai for initiating the investigation and technical assistance and Drs Susan Martinis and Paul Fox for technical guidance. We also thank Dr Hui Xu and the Tumor Engineering and Phenotyping Shared Resource at the Cancer Center of Illinois for expert assistance with cancer cell culture and tumor histology.

Funding and additional information—This work was supported by grants from the National Institutes of Health (grant nos.: CA288207 [to E. R. N.] and GM089771 [to J. C.]), Department of Defense Era of Hope Scholar Award (grant no.: BC200206/W81XWH-20-BCRP-EOHS [to E. R. N.]), and the Cancer Center at Illinois Graduate Cancer Scholarship Program Award (to S. V. B.). The content is solely the responsibility of the authors and does not necessarily represent the official views of the National Institutes of Health.

Author contributions—P. B., E. R. N., and J. C. conceptualization; P. B. and R. A. methodology; P. B. formal analysis; P. B., R. A., S. V. B., E. W., M. J. v. d. D., K. L. W., A. R.-.O., and E.R.N. investigation; P. B. and J. C. writing–original draft; P. B., R. A., S. V. B., E. W., M. J. v. d. D., K. L. W., A. R.-O., E. R. N., and J. C. writing–review & editing; P. B., R.A., S. V. B., A. R.-.O., and E. R. N. visualization; A. R.-O. and J.C. supervision; J. C. project administration; S. V. B., E. R. N., and J. C. funding acquisition.

Conflict of interest—The authors declare that they have no conflicts of interest with the contents of this article.

Abbreviations—The abbreviations used are: AAD, aminoacylation domain; AARS, aminoacyl-tRNA synthetase; ABD, anticodon-binding domain; co-IP, coimmunoprecipitation; ED, editing domain; EGFR, epidermal growth factor receptor; HEK293, human embryonic kidney 293 cell line; IL-6, interleukin 6; JAK, Janus kinase; NSCLC, non–small cell lung cancer; STAT3, signal transducer and activator of transcription 3; TARS1, threonyl-tRNA synthetase 1.

References

1. Darnell, J. E. (1997) STATs and gene regulation. *Science* **277**, 1630–1635
2. Levy, D. E., and Darnell, J. E., Jr. (2002) Stats: transcriptional control and biological impact. *Nat. Rev. Mol. Cell Biol.* **3**, 651–662
3. Philips, R. L., Wang, Y., Cheon, H., Kanno, Y., Gadina, M., Sartorelli, V., *et al.* (2022) The JAK-STAT pathway at 30: much learned, much more to do. *Cell* **185**, 3857–3876
4. Stark, G. R., and Darnell, J. E., Jr. (2012) The JAK-STAT pathway at twenty. *Immunity* **36**, 503–514
5. Yamaoka, K., Saharinen, P., Pesu, M., Holt, V. E., 3rd, Silvennoinen, O., and O'Shea, J. J. (2004) The Janus kinases (Jaks). *Genome Biol.* **5**, 253
6. Schindler, C., and Darnell, J. E., Jr. (1995) Transcriptional responses to polypeptide ligands: the JAK-STAT pathway. *Annu. Rev. Biochem.* **64**, 621–651
7. Sadowski, H. B., Shuai, K., Darnell, J. E., Jr., and Gilman, M. Z. (1993) A common nuclear signal transduction pathway activated by growth factor and cytokine receptors. *Science* **261**, 1739–1744
8. Silvennoinen, O., Schindler, C., Schlessinger, J., and Levy, D. E. (1993) Ras-independent growth factor signaling by transcription factor tyrosine phosphorylation. *Science* **261**, 1736–1739
9. Levy, D. E., and Lee, C. K. (2002) What does Stat3 do? *J. Clin. Invest.* **109**, 1143–1148
10. Leonard, W. J., and O'Shea, J. J. (1998) JAKS and STATS: biological implications. *Annu. Rev. Immunol.* **16**, 293–322
11. Decker, T., and Kovarik, P. (2000) Serine phosphorylation of STATs. *Oncogene* **19**, 2628–2637
12. Bromberg, J. F., Wrzeszczynska, M. H., Devgan, G., Zhao, Y., Pestell, R. G., Albanese, C., *et al.* (1999) Stat3 as an oncogene. *Cell* **98**, 295–303
13. Hu, Y., Dong, Z., and Liu, K. (2024) Unraveling the complexity of STAT3 in cancer: molecular understanding and drug discovery. *J. Exp. Clin. Cancer Res.* **43**, 23
14. Yu, H., Pardoll, D., and Jove, R. (2009) STATs in cancer inflammation and immunity: a leading role for STAT3. *Nat. Rev. Cancer* **9**, 798–809
15. Wang, H. Q., Man, Q. W., Huo, F. Y., Gao, X., Lin, H., Li, S. R., *et al.* (2022) STAT3 pathway in cancers: past, present, and future. *MedComm* **3**, e124
16. Johnson, D. E., O'Keefe, R. A., and Grandis, J. R. (2018) Targeting the IL-6/JAK/STAT3 signalling axis in cancer. *Nat. Rev. Clin. Oncol.* **15**, 234–248
17. Tanaka, T., Narazaki, M., and Kishimoto, T. (2014) IL-6 in inflammation, immunity, and disease. *Cold Spring Harbor Perspect. Biol.* **6**, a016295
18. Hirano, T. (2021) IL-6 in inflammation, autoimmunity and cancer. *Int. Immunol.* **33**, 127–148
19. Dutta, P., Sabri, N., Li, J., and Li, W. X. (2014) Role of STAT3 in lung cancer. *Jakstat* **3**, e999503
20. Mizuno, K., Sone, S., Orino, E., Nii, A., and Ogura, T. (1994) Autonomous expressions of cytokine genes by human lung cancer cells and their paracrine regulation. *Jpn. J. Cancer Res.* **85**, 179–186
21. Yanagawa, H., Sone, S., Takahashi, Y., Haku, T., Yano, S., Shinohara, T., *et al.* (1995) Serum levels of interleukin 6 in patients with lung cancer. *Br. J. Cancer* **71**, 1095–1098
22. Ibba, M., and Soll, D. (2000) Aminoacyl-tRNA synthesis. *Annu. Rev. Biochem.* **69**, 617–650
23. Guo, M., and Schimmel, P. (2013) Essential nontranslational functions of tRNA synthetases. *Nat. Chem. Biol.* **9**, 145–153
24. Guo, M., Yang, X. L., and Schimmel, P. (2010) New functions of aminoacyl-tRNA synthetases beyond translation. *Nat. Rev. Mol. Cell Biol* **11**, 668–674
25. Kwon, N. H., Fox, P. L., and Kim, S. (2019) Aminoacyl-tRNA synthetases as therapeutic targets. *Nat. Rev. Drug Discov.* **18**, 629–650
26. Yao, P., Poruri, K., Martinis, S. A., and Fox, P. L. (2014) Non-catalytic regulation of gene expression by Aminoacyl-tRNA synthetases. In: Kim, S., ed. *Aminoacyl-tRNA Synthetases in Biology and Medicine*, Springer Netherlands, Dordrecht: 167–187
27. Barai, P., and Chen, J. (2024) Beyond protein synthesis: non-translational functions of threonyl-tRNA synthetases. *Biochem. Soc. Trans.* **52**, 661–670
28. Jeong, S. J., Park, S., Nguyen, L. T., Hwang, J., Lee, E. Y., Giong, H. K., *et al.* (2019) A threonyl-tRNA synthetase-mediated translation initiation machinery. *Nat. Commun.* **10**, 1357
29. Dai, C., Reyes-Ordonez, A., You, J.-S., and Chen, J. (2021) A non-translational role of threonyl-tRNA synthetase in regulating JNK signaling during myogenic differentiation. *FASEB J.* **35**, e21948
30. Williams, T. F., Mirando, A. C., Wilkinson, B., Francklyn, C. S., and Lounsbury, K. M. (2013) Secreted Threonyl-tRNA synthetase stimulates endothelial cell migration and angiogenesis. *Sci. Rep.* **3**, 1317
31. Uhlén, M., Fagerberg, L., Hallström, B. M., Lindskog, C., Oksvold, P., Mardinoglu, A., *et al.* (2015) Proteomics. Tissue-based map of the human proteome. *Science* **347**, 1260419
32. Lánczky, A., and Győrffy, B. (2021) Web-Based survival analysis tool tailored for medical research (KMplot): development and implementation. *J. Med. Internet Res.* **23**, e27633
33. Chen, Y., Ruan, Z.-R., Wang, Y., Huang, Q., Xue, M.-Q., Zhou, X.-L., *et al.* (2018) A threonyl-tRNA synthetase-like protein has tRNA aminoacylation and editing activities. *Nucleic Acids Res.* **46**, 3643–3656
34. Besser, D., Bromberg, J. F., Darnell, J. E., and Hanafusa, H. (2023) A single amino acid substitution in the v-Eyk intracellular domain results in activation of Stat3 and enhances cellular transformation. *Mol. Cell Biol.* **19**, 1401–1409
35. Song, L., Rawal, B., Nemeth, J. A., and Haura, E. B. (2011) JAK1 activates STAT3 activity in non-small-cell lung cancer cells and IL-6 neutralizing antibodies can suppress JAK1-STAT3 signaling. *Mol. Cancer Ther.* **10**, 481–494
36. Xu, Y., Jin, J., Xu, J., Shao, Y. W., and Fan, Y. (2017) JAK2 variations and functions in lung adenocarcinoma. *Tumour Biol.* **39**, 1010428317711140

37. Zhang, J., Xu, Q., and Sun, G. (2025) Lipocalin-2 promotes NSCLC progression by activating the JAK2/STAT3 signaling pathway. *J. Transl Med.* **23**, 419
38. Pardanani, A., Lasho, T., Smith, G., Burns, C. J., Fantino, E., and Tefferi, A. (2009) CYT387, a selective JAK1/JAK2 inhibitor: in vitro assessment of kinase selectivity and preclinical studies using cell lines and primary cells from polycythemia vera patients. *Leukemia* **23**, 1441–1445
39. Tsherniak, A., Vazquez, F., Montgomery, P. G., Weir, B. A., Kryukov, G., Cowley, G. S., *et al.* (2017) Defining a cancer dependency map. *Cell* **170**, 564–576.e16
40. Cai, Z., Apolinario, S., Baiao, A. R., Pacini, C., Sousa, M. D., Vinga, S., *et al.* (2024) Synthetic augmentation of cancer cell line multi-omic datasets using unsupervised deep learning. *Nat. Commun.* **15**, 10390
41. Park, S. G., Ewalt, K. L., and Kim, S. (2005) Functional expansion of aminoacyl-tRNA synthetases and their interacting factors: new perspectives on housekeepers. *Trends Biochem. Sci.* **30**, 569–574
42. Rubio Gomez, M. A., and Ibba, M. (2020) Aminoacyl-tRNA synthetases. *Rna* **26**, 910–936
43. Wen, Z., Zhong, Z., and Darnell, J. E., Jr. (1995) Maximal activation of transcription by Stat1 and Stat3 requires both tyrosine and serine phosphorylation. *Cell* **82**, 241–250
44. Coelho, M. A., Cooper, S., Strauss, M. E., Karakoc, E., Bhosle, S., Gonçalves, E., *et al.* (2023) *Base editing screens map mutations affecting interferon-γ signaling in cancer. Cancer Cell* **41**, 288–303.e6
45. Stewart, S. A., Dykxhoorn, D. M., Palliser, D., Mizuno, H., Yu, E. Y., An, D. S., *et al.* (2003) Lentivirus-delivered stable gene silencing by RNAi in primary cells. *RNA* **9**, 493–501
46. Son, K., You, J.-S., Yoon, M.-S., Dai, C., Kim, J. H., Khanna, N., *et al.* (2019) *Nontranslational function of leucyl-tRNA synthetase regulates myogenic differentiation and skeletal muscle regeneration. J. Clin. Invest.* **129**, 2088–2093
47. Vidana Gamage, H. E., Albright, S. T., Smith, A. J., Farmer, R., Shahoei, S. H., Wang, Y., *et al.* (2024) *Development of NR0B2 as a therapeutic target for the re-education of tumor associated myeloid cells. Cancer Lett.* **597**, 217086
48. Vidana Gamage, H. E., Shahoei, S. H., Wang, Y., Jacquin, E., Weisser, E., Bautista, R. O., *et al.* (2024) *NR0B2 re-educates myeloid immune cells to reduce regulatory T cell expansion and progression of breast and other solid tumors. Cancer Lett.* **597**, 217042
49. Nelczyk, A. T., Ma, L., Gupta, A. D., Gamage, H. E. V., McHenry, M. T., Henn, M. A., *et al.* (2022) *The nuclear receptor TLX (NR2E1) inhibits growth and progression of triple- negative breast cancer. Biochim. Biophys. Acta Mol. Basis Dis.* **1868**, 166515
50. Halawani, D., Gogonea, V., DiDonato, J. A., Pipich, V., Yao, P., China, A., *et al.* (2018) *Structural control of caspase-generated glutamyl-tRNA synthetase by appended noncatalytic WHEP domains. J. Biol. Chem.* **293**, 8843–8860

Pallob Barai is a PhD candidate in the Department of Cell and Developmental Biology at the University of Illinois Urbana-Champaign. His research investigates non-translational functions of aminoacyl-tRNA synthetases in cell signaling and muscle-derived cytokine function in skeletal muscle regeneration. He focuses on how threonyl-tRNA synthetase 1 (TARS1) operates beyond protein synthesis to modulate the JAK–STAT pathway, aiming to identify actionable molecular mechanisms that can inform future therapeutic strategies.

Reean Abdullah is a graduate student at the Department of Cell & Developmental Biology at the University of Illinois Urbana-Champaign. She is currently studying the regulatory mechanisms of Rho guanine nucleotide exchange factors and the non-canonical roles of aminoacyl-tRNA synthetases. She first became interested in cancer signaling while engineering oncogenic gene fusions in leukemia as an undergraduate. Work from this study opens a promising avenue for targeting aberrantly amplified signaling pathways in cancer. LinkedIn profile link: https://www.linkedin.com/in/reean-raisa-abdullah/.

SUPPORTING INFORMATION – MATERIALS AND METHODS

Antibodies

Antibodies for the following proteins were obtained from Cell Signaling Technology (Danvers, MA, USA): STAT3 (#12640), phospho-STAT3 (Y705; #9138), phospho-STAT3 (S727; #9134), JAK2 (#3230), phospho-JAK2 (#3776), ERK1/2 (#4695), phospho-ERK1/2 (Thr202/Tyr204; #4370), p38 MAPK (#9212), phospho-p38 MAPK (Thr180/Tyr182; #4511), AKT (#9272), phospho-AKT (Thr308; #9275), S6K1 (#34475), phospho-S6K1 (Thr389; #9243). Antibodies for TARS1 were obtained from Abcam (Cambridge, MA, USA. #ab236903) and Santa Cruz Biotechnology (#sc-166211). Anti-Flag antibodies were from Sigma-Aldrich (for immunofluorescence, #F9219) and Proteintech (for western blotting, #20543-1-AP). Anti-GFP (#66002-1-Ig) and anti-tubulin (#80762-1-RR) antibodies were from Proteintech.

Plasmids

pcDNA3-Flag-TARS1 (mouse cDNA) was previously reported [1], and was used to generate all point mutants of TARS1 using the Q5® Site-Directed Mutagenesis Kit (New England Biolabs, Ipswich, MA, USA) and truncation mutants using PCR. GFP-TARS1, GFP-DARS1, GFP-KARS1, and GFP-EPRS were created by subcloning human cDNAs into pcDNA3-EGFP, a gift from Doug Goldenbock (Addgene, plasmid #13031). GFP-LARS1 was purchased from Sino Biological (LARS1-GFP-Spark). All the constructs above have GFP at the C-terminus. Human STAT3 cDNA was a gift from the laboratory of James Darnell [2] and then subcloned into pcDNA3-Flag or pcDNA3-EGFP described above. The following plasmids were obtained from Addgene (Watertown, MA, USA): STAT3-C-Flag (#8722, [3]) and STAT3 luciferase reporter (4x M67 pTATA Tk-Luc) (#8688, [4]) were gifts from James Darnell; Flag-JAK1 (#174572, [5]) was a gift from Mathew Garnett; pCMV-dR8.2 dvpr (#8455, [6]) and pCMV-VSV-G (#8454, [6]) were gifts from Robert Weinberg.

Cell culture and transfection

All cell lines used in this study were originally obtained from ATCC and authenticated by the Tumor Engineering and Phenotyping Shared Resource at the Cancer Center of Illinois. Cells were monitored for mycoplasma contamination regularly, and all cells were mycoplasma-negative except for HEK293 cells used for the co-IP experiments. Transfection of H1703 cells was performed using Lipofectamine ^{TM} 3000 (Invitrogen, # L3000008) in 12-well plates. Briefly, 1 µg of plasmid DNA was mixed with 2 µL of P3000 in 100 µL Opti-MEM^{TM}, then combined with 1 µL of Lipofectamine 3000. After 15-min incubation at room temperature, the mixture was added to the cells. Medium was replaced after 4 hrs and cells were collected 72 hrs post-transfection. For experiments in HEK293, cells were transfected in 12-well or 6-cm plates using polyethylenimine (PEI) at 3 µL/µg of DNA. The DNA:PEI mixture was incubated at room temperature for 15 min before adding to the cells.

Lentivirus-delivered RNA interference

shRNA in the pLKO.1-puro vector targeting human TARS1 was previously reported [1] and obtained from Sigma-Aldrich (clone ID: TRCN0000045680). A hairpin of scrambled sequence (shScramble) used for a negative control and lentivirus packaging plasmids were previously described [7]. For lentiviral packaging, pLKO-shRNA DNA, pCMV-dR8.2 dvpr, and pCMV-VSV-G were co-transfected at 4 µg, 3.6 µg, and 0.4 µg into HEK293T cells using polyethyleneimine (PEI) (Avantor-VWR, AAA43896-01) in a 10-cm plate. The medium was changed 6-8 hrs post-transfection, and the medium containing viruses was collected 24–48 hrs post-transfection. NSCLC cell lines were transduced in growth medium with virus plus 8 µg/mL polybrene and selected in 2 µg/mL puromycin for 48–96 hrs, followed by re-seeding into 12-well plates.

Cell viability assay

Cells were trypsinized to harvest and resuspended in an appropriate volume of culture medium. An equal volume of 0.4% Trypan Blue solution (Thermo Fisher Scientific, #15250061) was mixed with the cell suspension and incubated for 2-3 min at room temperature. The mixture was then loaded onto a hemocytometer, and viable (unstained) cells were counted under a light microscope. Each sample was counted in duplicate to ensure accuracy.

Cell proliferation assay

To assess cell proliferation, EdU labeling was performed as previously described [8]. Briefly, after 96 hrs of selection in puromycin, H1703 cells were incubated with EdU (final concentration 1 μM) for 4 hrs. Upon fixation with 3.7% formaldehyde, cells were treated with PBS containing 10 μM FAM azide 5-isomer, 1 mM CuSO4, and 100 mM ascorbic acid for 30 min, followed by DAPI staining for 30 min. Cells were imaged with a Leica DMI 4000B fluorescence microscope (Leica, Wetzlar, Germany). The fluorescence images were captured using a RETIGA EXi camera (QImaging, Surry, BC, Canada) and Image Pro Express software (Media Cybernetics, Rockville, MD, USA). Images were analyzed using ImageJ (NIH, https://imagej-nih-gov.proxy2.library.illinois.edu/ij/).

TUNEL assay

To assess apoptosis, cells were fixed using 3.7% formaldehyde and TUNEL assays were performed using the Click-iT™ TUNEL Alexa Fluor Imaging Assay Kit (Thermo Fisher Scientific, #C10245) according to the manufacturer's instructions. Fluorescence microscopy and quantification were performed as described in "Cell proliferation assay" above.

Mouse xenograft

Female athymic nude mice were purchased from Charles River Laboratories and grafted with H1703 derivative cell lines into the flank. Assessment for palpable tumors occurred at least two times per week post-graft and resulting tumor sizes were measured with calipers as we have done previously [9-11]. Data of tumor-free survival was presented as time to first palpable tumor in a Kaplan-Meier survival curve and subjected to log-rank (Mantel-Cox) test for statistical analysis. Tumors were resected after reaching at least ~1000 mm^3 or when excessive scratching by the animal occurred. Resected tumors were fixed in formaldehyde, transferred to 70% ethanol, embedded in paraffin, and sectioned, followed by hematoxylin and eosin (H&E) staining for histological analysis.

Luciferase assay

H1703 cells grown in 12-well plates were transduced with either shScramble or shTARS1 lentivirus and selected for 48 hrs in 2 μg/ml puromycin. Cells of equal numbers were then plated on fresh plates in growth medium. Next day, cells were transfected with the STAT3 reporter plasmid for 48 hrs. For rescue experiments, empty vector, WT-TARS1 or mutants were co-transfected with the reporter plasmid. Cells were lysed with 1x passive lysis buffer (#E1910, Promega, Madison, WI, USA) under gentle shaking at room temperature for 15 min. The lysate was cleared in a microcentrifuge (17000 rpm; 30 sec), and the supernatant was subjected to assay using the Luciferase Reporter Assay System (Cat #E1500, Promega, Madison, WI, USA) on an Agilent BioTek Synergy LX Multimode plate reader.

Immunofluorescence staining

H1703 cells were seeded on a 12-well plate in growth medium after 48 hrs of puromycin selection upon TARS1 knockdown. Cells were transfected with either WT or mutant Flag-TARS1 for 72 hrs. After transfection cells were incubated with EdU (final concentration 1 μM) for 4 hrs. Samples were fixed using 3.7% formaldehyde. EdU signals were developed using the method

described above, followed by immunostaining with an anti-Flag antibody. Briefly, cells were permeabilized with 0.2% Triton X-100 for 10 min following a 30-min block with 5% bovine serum albumin (BSA). Samples were then incubated with an anti-Flag antibody (1:100) for 2 hrs at room temperature. After rinsing with PBS containing 0.05% tween-20 (PBST), secondary antibody (Alexa Fluor 594-conjugated anti-mouse IgG, 1:50) was applied for 1 hr. Samples were washed three times with PBST, counterstained with DAPI, and imaged. Fluorescence microscopy and image analysis were performed as described in the "Cell proliferation assay" section above. Flag-positive and Flag-negative cells on the same images were quantified separately for EdU signals to determine proliferation of transfected and non-transfected cells, respectively.

Cell lysis and western blotting

For western blotting, cells were rinsed with PBS and lysed in SDS sample buffer containing 5% β-mercaptoethanol. Proteins were resolved on SDS-PAGE, transferred onto PVDF membrane (EMD Millipore, Darmstadt, Germany), and incubated with various antibodies according to the manufacturers' recommendations. Detection of horseradish peroxidase-conjugated secondary antibodies was performed with SuperSignal West Pico PLUS Chemiluminescent Substrate (Thermo Fisher Scientific, Waltham, MA, USA) and visualized using an iBright CL1000 or CL1500 Imaging System (Thermo Fisher Scientific). Quantification of western results were performed by densitometry in ImageJ (NIH, https://imagej-nih-gov.proxy2.library.illinois.edu/ij/). Equal loading of protein samples within an experiment on a protein gel was confirmed by blotting for tubulin as a house-keeping protein in lysates. However, we note that tubulin has not been validated to be unaffected by all experimental conditions in this study. Tubulin levels were not used for quantification of data except for Fig. 1A and Fig. S2A. The activity of each signaling protein was expressed as the ratio of phosphorylation level to total level of that protein, independent of the tubulin level.

Immunoprecipitation

HEK293 cells were seeded in 6-cm dishes at 60-80% confluency, transfected for 48 hrs, followed by lysis in 20 mM Tris (pH 7.5), 2 mM EDTA, 2 mM EGTA, 0.1 mM Na_3VO_4, 25 mM NaF, 25 mM β-glycerophosphate, 150 mM NaCl, 1% NP-40, and 1x Protease inhibitor cocktail (Sigma-Aldrich; Cat #P8340). The cell lysates were cleared with a microcentrifuge at 13,000 rpm for 7 min at 4 °C. Flag-tagged proteins were immunoprecipitated from the lysates by 20-min incubation with anti-FLAG M2 Affinity Gel (Sigma-Aldrich; #A2220) followed by three washes with 500 µL lysis buffer each. The beads were resuspended in SDS sample buffer and heated at 95 °C for 5 min, followed by SDS-PAGE and western blotting. For immunoprecipitation of endogenous proteins, H1703 cells were seeded in 6-cm dishes at 85% confluency, followed by lysis in the aforementioned buffer and cleared by centrifugation. The cleared lysate was incubated with antibodies at 4 °C overnight, followed by incubation with Protein A agarose at 4 °C for 2 hrs. The beads were washed three times with the lysis buffer and then boiled in SDS sample buffer.

Aminoacylation assay

HEK293 cells were transfected with Flag-TARS1 (WT or mutants) or empty vector for 24 hrs. Cell lysates were subjected to anti-Flag immunoprecipitation as described above. The first wash was done in the cell lysis buffer, and the second wash was in 25 mM Tris-HCl pH 7.4, 150 mM NaCl, 1% NP-40, and 5% glycerol. tRNA aminoacylation assay was performed following a published protocol [12] with some modifications. To the immunocomplex on beads, 20 µL assay buffer was added containing 20 mM HEPES (pH 8.0), 100 mM NaCl, 5mM $MgCl_2$, 3mM ATP, 1mM DTT, and 20 µg/µL yeast tRNA. The reaction mixture was equilibrated to 30 °C in a thermomixer (Eppendorf), and the reaction was initiated by the addition of ^{3}H-threonine (with unlabeled threonine) to a final concentration of 150 µM. Following incubation at 30 °C for 30 min under gentle agitation, 10-µL aliquots were spotted on filter pads (Whatman®; #1003323) pre-soaked

with 10% trichloroacetic acid (TCA) and 0.5% Casamino acids. The filters were washed three times for 10 mins each with cold 5% TCA solution, followed by a brief rinse once with cold 70% ethanol and once with anhydrous ether. The washed pads were then dried under a heat lamp. Radioactivity was determined by liquid scintillation counting (Beckman Coulter LS 6500). Activity of the recombinant protein was calculated by subtracting the background (empty vector sample) and normalizing to WT-TRAS1 as 100%.

References

1. Dai, C., A. Reyes-Ordonez, J.-S. You, and J. Chen, *A non-translational role of threonyl-tRNA synthetase in regulating JNK signaling during myogenic differentiation.* **FASEB J**, 2021. 35: p. e21948.
2. Wen, Z., Z. Zhong, and J.E. Darnell, Jr., *Maximal activation of transcription by Stat1 and Stat3 requires both tyrosine and serine phosphorylation.* **Cell**, 1995. 82(2): p. 241-50.
3. Bromberg, J.F., M.H. Wrzeszczynska, G. Devgan, Y. Zhao, R.G. Pestell, C. Albanese, and J.E. Darnell, Jr., *Stat3 as an oncogene.* **Cell**, 1999. 98(3): p. 295-303.
4. Besser, D., J.F. Bromberg, J.E. Darnell, and H. Hanafusa, *A Single Amino Acid Substitution in the v-Eyk Intracellular Domain Results in Activation of Stat3 and Enhances Cellular Transformation.* **Molecular and Cellular Biology**, 2023. 19(2): p. 1401-1409.
5. Coelho, M.A., S. Cooper, M.E. Strauss, E. Karakoc, S. Bhosle, E. Gonçalves, G. Picco, T. Burgold, C.M. Cattaneo, V. Veninga, S. Consonni, C. Dinçer, S.F. Vieira, F. Gibson, S. Barthorpe, C. Hardy, J. Rein, M. Thomas, J. Marioni, E.E. Voest, A. Bassett, and M.J. Garnett, *Base editing screens map mutations affecting interferon-γ signaling in cancer.* **Cancer Cell**, 2023. 41(2): p. 288-303.e6.
6. Stewart, S.A., D.M. Dykxhoorn, D. Palliser, H. Mizuno, E.Y. Yu, D.S. An, D.M. Sabatini, I.S. Chen, W.C. Hahn, P.A. Sharp, R.A. Weinberg, and C.D. Novina, *Lentivirus-delivered stable gene silencing by RNAi in primary cells.* **RNA**, 2003. 9(4): p. 493-501.
7. Stewart, S.A., D.M. Dykxhoorn, D. Palliser, H. Mizuno, E.Y. Yu, D.S. An, D.M. Sabatini, I.S.Y. Chen, W.C. Hahn, P.A. Sharp, R.A. Weinberg, and C.D. Novina, *Lentivirus-delivered stable gene silencing by RNAi in primary cells.* **Rna**, 2003. 9(4): p. 493-501.
8. Son, K., J.-S. You, M.-S. Yoon, C. Dai, J.H. Kim, N. Khanna, A. Banerjee, S.A. Martinis, G. Han, J.M. Han, S. Kim, and J. Chen, *Nontranslational function of leucyl-tRNA synthetase regulates myogenic differentiation and skeletal muscle regeneration.* **Journal of Clinical Investigation**, 2019. 129(5): p. 2088-2093.
9. Vidana Gamage, H.E., S.T. Albright, A.J. Smith, R. Farmer, S.H. Shahoei, Y. Wang, E.C. Fink, E. Jacquin, E. Weisser, R.O. Bautista, M.A. Henn, C.P. Schane, A.T. Nelczyk, L. Ma, A. Das Gupta, S.V. Bendre, T. Nguyen, S. Tiwari, N. Krawczynska, S. He, E. Tjoanda, H. Chen, M. Sverdlov, P.H. Gann, R. Boidot, F. Vegran, S.W. Fanning, L. Apetoh, P.J. Hergenrother, and E.R. Nelson, *Development of NR0B2 as a therapeutic target for the re-education of tumor associated myeloid cells.* **Cancer Lett**, 2024. 597: p. 217086.
10. Vidana Gamage, H.E., S.H. Shahoei, Y. Wang, E. Jacquin, E. Weisser, R.O. Bautista, M.A. Henn, C.P. Schane, A.T. Nelczyk, L. Ma, A. Das Gupta, S.V. Bendre, T. Nguyen, S. Tiwari, E. Tjoanda, N. Krawczynska, S. He, S.T. Albright, R. Farmer, A.J. Smith, E.C. Fink, H. Chen, M. Sverdlov, P.H. Gann, R. Boidot, F. Vegran, S.W. Fanning, P.J. Hergenrother, L. Apetoh, and E.R. Nelson, *NR0B2 re-educates myeloid immune cells to*

reduce regulatory T cell expansion and progression of breast and other solid tumors. **Cancer Lett**, 2024. 597: p. 217042.
11. Nelczyk, A.T., L. Ma, A.D. Gupta, H.E.V. Gamage, M.T. McHenry, M.A. Henn, M. Kadiri, Y. Wang, N. Krawczynska, S. Bendre, S. He, S.H. Shahoei, Z. Madak-Erdogan, S.H. Hsiao, T. Saleh, V. Carpenter, D.A. Gewirtz, M.J. Spinella, and E.R. Nelson, *The nuclear receptor TLX (NR2E1) inhibits growth and progression of triple- negative breast cancer.* **Biochim Biophys Acta Mol Basis Dis**, 2022. 1868(11): p. 166515.
12. Halawani, D., V. Gogonea, J.A. DiDonato, V. Pipich, P. Yao, A. China, C. Topbas, K. Vasu, A. Arif, S.L. Hazen, and P.L. Fox, *Structural control of caspase-generated glutamyl-tRNA synthetase by appended noncatalytic WHEP domains.* **J Biol Chem**, 2018. 293(23): p. 8843-8860.

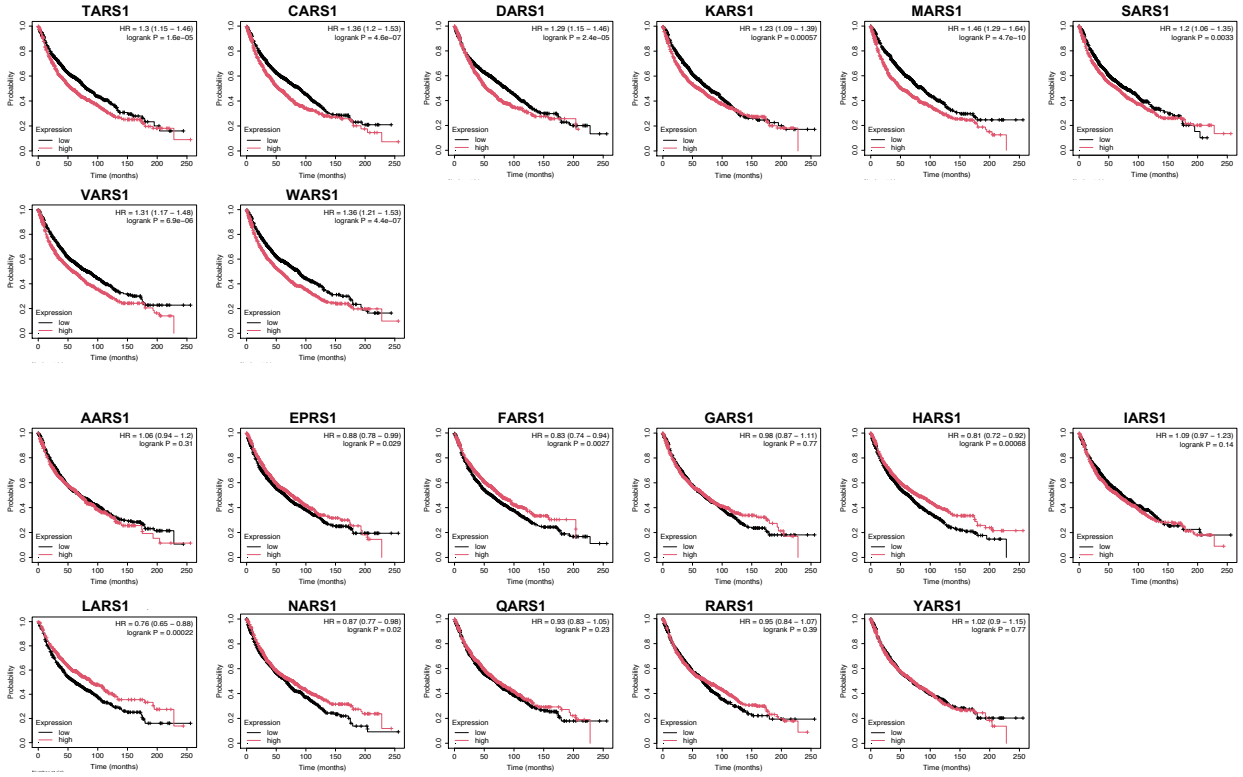

Figure S1: AARS expression and patient survival in lung cancer
KM-plots for all AARSs in lung cancer are shown, separated into two groups – high expression correlates with poor patient overall survival (upper group) or not (lower group).

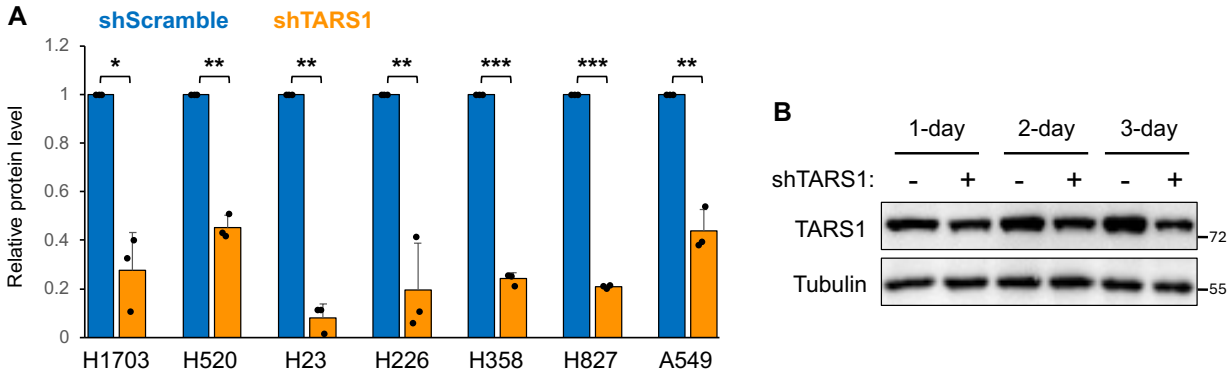

Figure S2: TARS1 knockdown efficiency

(A) Various cell lines were transduced by lentivirus shScramble or shTARS1 overnight, selected in puromycin for 4 days, and then subjected to western blot analysis followed by densitometry quantification. Data were normalized to shScramble for each cell line. N = 3. One-sample t-test was performed. *$p < 0.05$, **$p < 0.01$, ***$p<0.001$.

(B) H1703 cells were transduced by lentivirus shScramble or shTARS1 overnight, and selected in puromycin for 1, 2, or 3 days, followed by western blot analysis. Results shown are representative of 3 independent experiments.

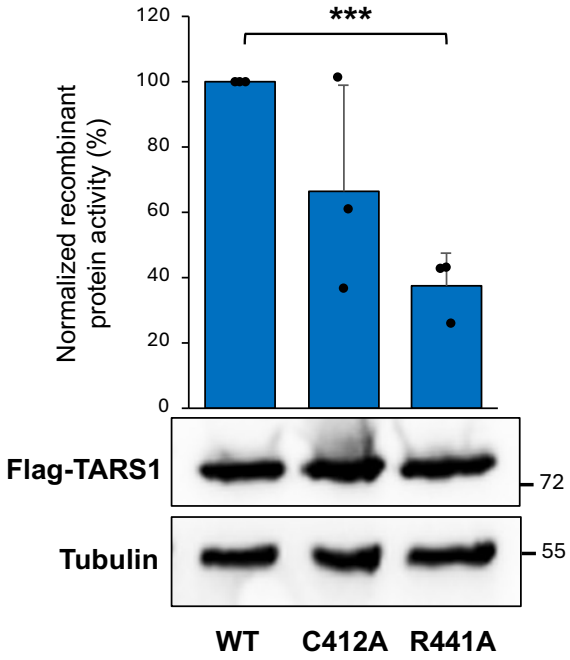

Figure S3: Aminoacylation assay
HEK293 cells were transfected with Flag-tagged WT or mutant TARS1 for 24 hours, followed by cell lysis and anti-Flag IP. The immunocomplexes were subjected to tRNA aminoacylation assay, and activities were normalized to WT as 100%. N = 3. One-sample t-test: ***$p < 0.001$.

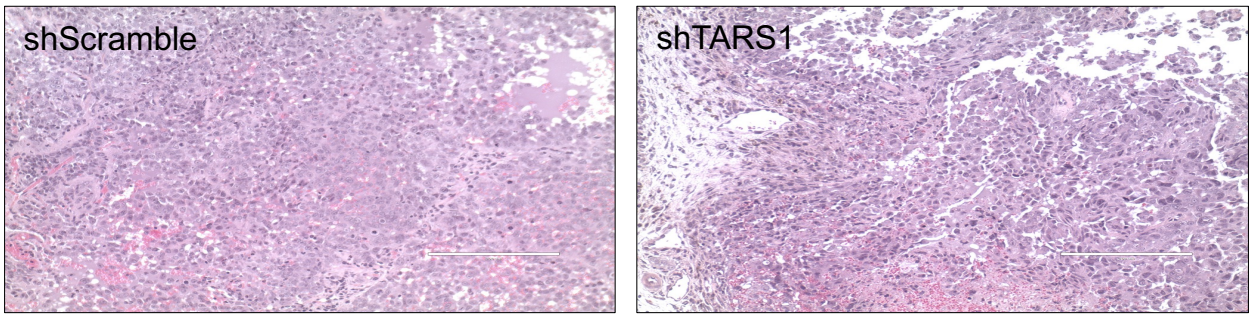

Figure S4: Histology of xenographed tumors
H&E images of representative tumors from Fig. 1F are shown. Scale bars: 200 μm.

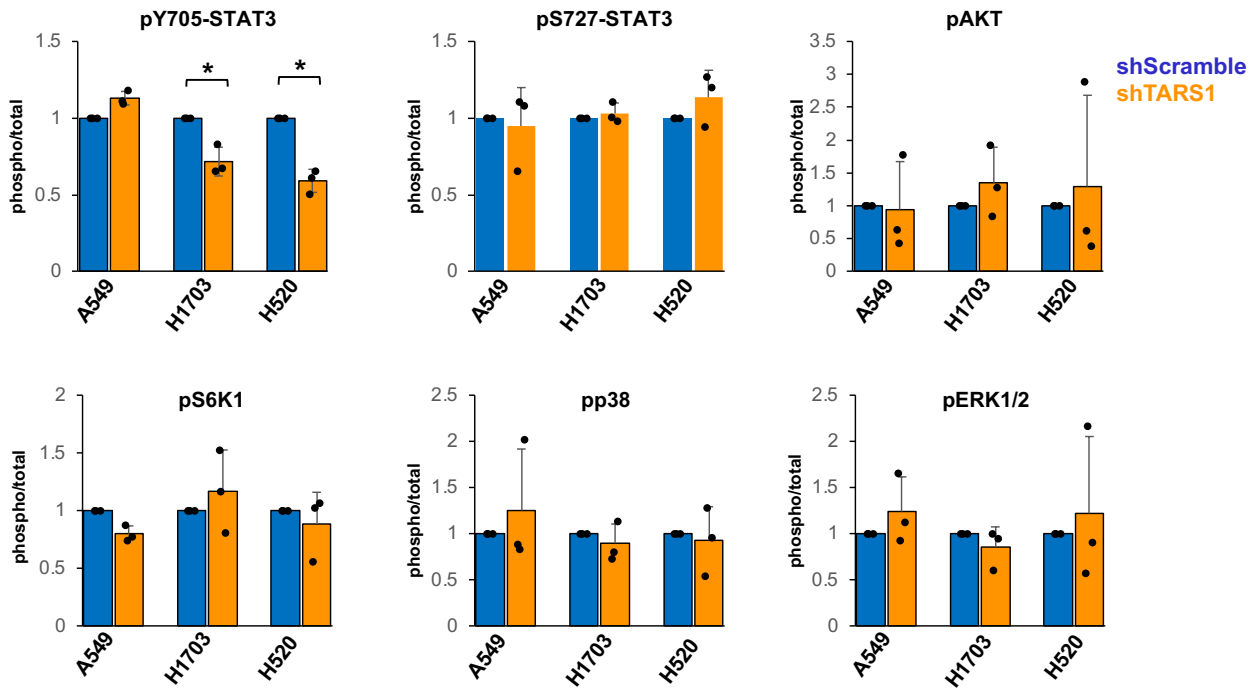

Figure S5: TARS1 knockdown effects on signaling proteins
Densitometric quantification of western blots shown in Fig. 2A. Data were normalized to shScramble for each cell line. N = 3. One sample t-test was performed. *$p < 0.05$.

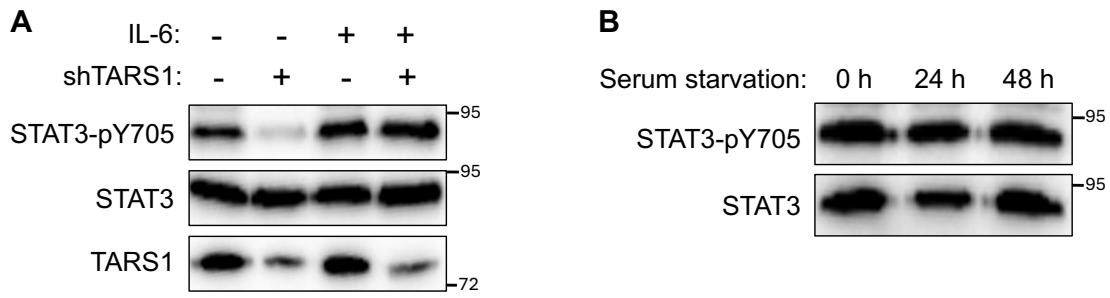

Figure S6: TARS1 activation of STAT3 in H1703 cells is independent of upstream signals
(A) H1703 cells were transduced by lentivirus shScramble (-) or shTARS1 (+) overnight, selected in puromycin for 4 days, and then stimulated with 10 nM IL-6 for 30 min followed by western analysis. Results shown are representative of 3 independent experiments.
(B) H1703 cells were cultured in serum-free medium for 24 or 48 hours, followed by western analysis. Results shown are representative of 3 independent experiments.

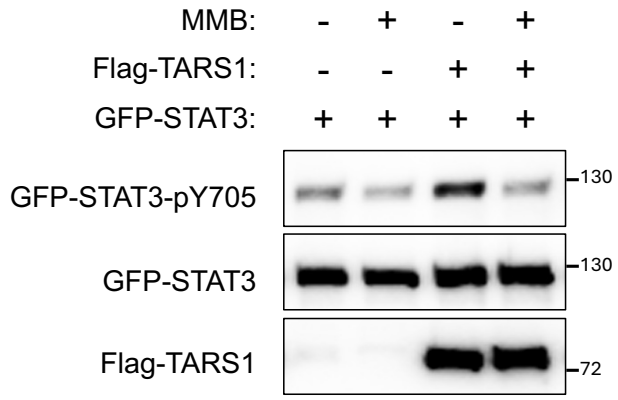

Figure S7: TARS1 activation of STAT3 is dependent on JAK activity
HEK293 cells were transfected with GFP-STAT3 with or without Flag-TARS1 for 48 hours, followed by treatment with 2.5 μM momelotinib (MMB) or DMSO for 60 mins. Western blots shown are representative of 3 independent experiments.